Partitioning and Diffusion Studies of Bodipy-Fingolimod Analogs, Immune Suppressors, in Mouse Embryonic Fibroblast Cells

A THESIS
SUBMITTED TO THE FACULTY OF THE GRADUATE SCHOOL
OF THE UNIVERSITY OF MINNESOTA
BY

W.P.M. Dhanushka Wickramasinghe

IN PARTIAL FULFILLMENT OF THE REQUIREMENTS
FOR THE DEGREE OF
MASTER OF SCIENCE

Thesis Advisor: Ahmed A. Heikal

December 2011

Acknowledgements

First I would like to pay my sincere gratitude to my advisor, Dr. Ahmed Heikal, for his continuous support and guidance throughout my graduate study. I would also like to thank my thesis advisors, Dr. Steven Berry and Dr. Clay Carter, not only for their valuable time, but also being such a good influence on me.

I would also like to thank Dr. Erin Sheets and Virginia Haynes and also my dear colleagues, Peter Steltz, Jillian Bartusek, Alex Paffrath, Jacob Stevens, and Rochelle Warner for their support. I really enjoyed working with you all and wish you all the best. Furthermore, my special thanks go to Dr. Joseph Johnson and Dr. Anne Hinderliter, for sharing their resources with us.

I am grateful to my parents and my brother, whom I miss so much, for giving me their love and blessing and also my husband, Kuravi, who always stands by me like a shadow and gives me encouragement. I would like to say how much we appreciate the computational work you've done for us even without being a member in the Heikal group. I cannot forget Mary and Paul Treuer, our host family. I am grateful to you for giving us a place in your hearts.

Last but not least, I would like to thank the Department of Chemistry and Biochemistry of University of Minnesota Duluth for giving me the opportunity to continue my studies in chemistry, all the professors I came across in my graduate student life. You are the best professors a student could ever have.

Dedication

I dedicate this dissertation to my loving parents, brother and husband.

Abstract

Sphingosine-1-phosphate is a bioactive signaling molecule that mediates important cellular functions such as cell proliferation, cytoskeletal rearrangement, angiogenesis, mobilization of intracellular calcium and immune cell trafficking. FTY720, a synthetic analog of sphingosine that has immunosuppressive properties, is the first oral drug approved by the U.S. FDA for treatment of multiple sclerosis (under the trade name Gilenya^{TM}). This thesis project is focused on the cellular uptake, partitioning, and diffusion studies on a fluorescent analog of this drug (namely, Bodipy-FTY720) in cultured C3H10T1/2 cells, derived from mouse embryos. Our working hypothesis is that Bodipy-FTY720 will be phosphorylated by sphingosine kinase 2 (SphK2) prior to binding to sphingosine-1-phosphate receptor 1 (S1PR1) followed by internalization and degradation of the receptor. Our results indicate that Bodipy-FTY720 resides in the endoplasmic reticulum (ER) of C3H10T1/2 cells and is excluded from the nucleus. Our single-molecule diffusion measurements also indicate that Bodipy-FTY720 binds with the cellular ER membrane prior to its phosphorylation, secretion via the ABC transporter, and then binding to S1PR1 receptors. These studies represent a step forward towards elucidating the action mechanism of FTY720 at the single-cell level.

Table of Contents

List of Tables

List of Figures

List of Abbreviations

1P	one photon
2P	two photon
ABC	ATP-binding cassette
APD	avalanche photodiode
ATCC	American Type Culture Collection
ATP	adenine triphosphate
BME	Eagle's Basal Medium
Bodipy	boron dipyrromethene or 4,4-difluoro-4-bora-3a,4a-diaza-s-indacene
BS	beam splitter
CNS	central nervous system
CW	continuous wavelength
DHS	dihydrosphingosine
DIC	differential interference contrast
DMSO	Dimethyl sulfoxide
EDG	endothelial differentiation gene
ER	endoplasmic reticulum
FBS	Fetal Bovine Serum
FCS	fluorescence correlation spectroscopy
FDA	Food and Drug Administration

FITC	Fluorescein isothiocyanate
FLIM	fluorescence lifetime imaging spectroscopy
FRET	fluorescence resonance energy transfer
FTY720	2-amino-2-[2-(4-octylphenyl)ethyl]-1,3-propanediol
GFP	green fluorescent protein
GPCR	G protein-coupled receptors
HEPES	4-(2-hydroxyethyl)-1-piperazineethanesulfonic acid
MCP-PMT	Microchannel plate photomultiplier tube
NA	numerical aperture
OI	oil immersion
PBS	phosphate buffered saline
S1P	sphingosine-1-phospate
S1PR	sphingosine-1-phospate receptor
SphK1/2	sphingosine kinase 1 or 2
SPT	Serine palmitoyltransferase
TIRF	total internal reflection fluorescence
TRITC	Tetramethyl rhodamine isothiocyanate
TCSPC	time correlated single photon counting
TXRED	texas red
WI	water immersion

List of Symbols

α	amplitude of fluorescence lifetime
β_i	pre-exponential factor (or amplitude fraction) of multiple exponential anisotropy decay
χ^2	chi square
δ	orientation angle between the absorbing and emitting dipoles
γ	number of excited photons
φ_i	rotational time
λ	wavelength
τ_i	fluorescence lifetime
τ_D	translational diffusion time
$< \tau_{fl} >$	average fluorescence lifetime
η	viscosity
ω_0	axial-to-lateral extension of the observation volume
ω_{xy}	lateral radius of the observation volume
N	number of molecules
D_T	translational diffusion coefficient
S	order parameter
r_o	initial anisotropy
t	time

T	temperature
R	universal gas constant
k_B	Boltzmann constant
V	hydrodynamic volume of a molecule
V_{app}	apparent hydrodynamic volume of a molecule

Chapter 1. Introduction

1.1 Sphingosine-1-phosphate Mediated GPCR signaling

Sphingosine-1-phosphate is a bioactive signaling molecule that mediates important cellular functions such as cell proliferation, cytoskeletal rearrangement, angiogenesis, mobilization of intracellular calcium and immune cell trafficking (1) (2). Sphingosine-1-phosphate is derived from the phosphorylation of Sphingosine, which is highly enriched in mammalian cellular membranes. *De novo* biosynthesis of sphingolipids is initiated at the outer leaflet of the endoplasmic reticulum (ER) (3). The first and rate-limiting step is catalyzed by serine palmitoyltransferase (SPT) to produce 3-ketodihydrosphingosine, which then reduced rapidly to dihydrosphingosine (DHS). Following N acylation, dihydroceramide is formed to yield ceramide, which can be further hydrolyzed by acid ceramidase to form sphingosine. Sphingosine is then phosphorylated and dephosphorylated by kinases and phosphatases, respectively. The phosphorylation of sphingosine, an ATP-dependent process, is carried out by sphingosine kinase 1 (SphK1) or sphingosine kinase 2 (SphK2) to produce sphingosine-1-phosphate (S1P). Dephosphorylation of S1P by Sphingosine phosphatase 1 or 2 (a magnesium dependent process) regulates the level of S1P in the cell. Another mechanism of S1P regulation is the irreversible degradation by sphingosine-1-phosphate lyase, which yields hexadecenal and phosphoethanolamine.

Sphingosine-1-phosphate acts as a ligand for five sphingosine-1-phosphate receptors ($S1PR_{1-5}$), which belong to endothelial differentiation gene (EDG) family G coupled protein receptors (GCPR) (4). Sphingosine-1-phosphate acts as a bioactive

metabolite in various cellular processes on the cell surface (*e.g.*, binding to the five receptors $S1PR_{1-5}$) and uncharacterized intracellular targets (Figure 1:1). S1P is also transported to extracellular milieu via ATP-binding cassette family transporters (ABC transporters), namely ABCC1 and ABCA1 (5) (6). These $S1PR_{1-5}$ receptors have been discovered in almost every tissue tested with different expression levels, which suggest biological functions (3) (Table 1:1). The phosphate group and the C3 hydroxyl group of S1P are believed to be significant for the binding specificity to these Shpingosine-1-phosphate receptors (7). Furthermore, the *D-erythro* configuration of S1P is essential for the high affinity in binding to these receptors. However, in recent computational studies, it has been shown that the hydroxyl group of S1P has the minimum contribution in S1P binding recognition to these receptors except in $S1PR_3$ (8).

Table 1:1 Physiological and biological functions of S1P Receptors.

S1P Receptor	Physiological Function
$S1P_1$	Blood vessel permeability, angiogenesis, immune cell egress from tissue cells, hematopoietic, vascular and stem cell survival, cytokine production
$S1P_2$	Blood vessel permeability, angiogenesis, blood pressure regulation, histamine clearance, recovery from anaphylaxis, inner ear development, perinatal survival
$S1P_3$	Perinatal survival, pulmonary epithelial integrity
$S1P_4$	Pematopoietic, vascular & stem cell survival, cytokine production
$S1P_5$	Immune cell egress from tissue cells, axon guidance

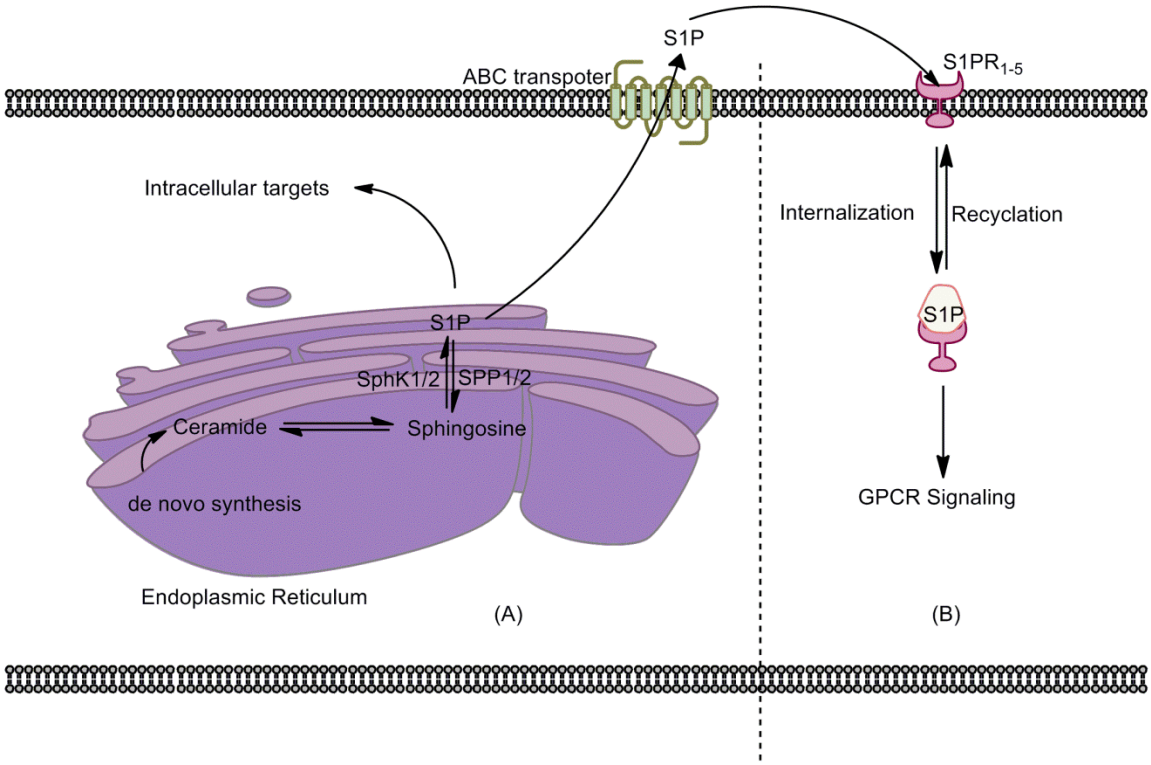

Figure 1:1 Sketch of the S1P signaling pathways. (A) Following its *de novo* synthesis in ER, Sphingosine is phosphorylated to produce Sphingosine-1-phosphate (S1P) by sphingosine kinases (SphK1 or SphK2) at the outer leaflet of the ER. S1P then participates either in intracellular targets or extracellular signaling pathways after being transported to the extracellular milieu by ABC transporter. Panel (B) shows the reversible internalization of S1P via $S1PR_{1-5}$ (see text).

1.2 Sphingosine-1-phosphate and Health

Sphingosine-1-phosphate has gained a lot of attention recently for its relation to the novel immunomodulator, FTY720, which is used to treat multiple sclerosis (MS). S1P plays a crucial role in MS-related processes that include inflammation and repair. During inflammation, S1P is released by platelets and can also be found in the serum at significant levels (9). $S1PR_1$ is known to be widely expressed in lymphocytes, which regulates the normal egress from lymph nodes (3). During such egress, T lymphocytes

migrate across the S1P gradient between lymph node and the afferent lymph. Under the normal immune response, activation of T cells in the lymph nodes causes an internalization of $S1P_1$ receptor (Figure 1:1- Panel B). After activation of T cells, $S1PR_1$ is recycled and re-circulated by the T cells to peripheral sites. In patients with MS, circulating auto aggressive T cells cross the blood brain barrier into the central nervous system (CNS) causing inflammation. This leads to the destruction of the myelin sheath that surrounds the axons as well as the loss of oligodendrocyte in great numbers causing demyelination, which ultimately cause the loss of axons and neurons. Although the CNS damage is usually self-repaired, the probability of recovery after repeated inflammation episodes is reduced causing tissue damage (10) and MS.

1.3 FTY720

The cause of MS, an autoimmune disease, is unknown and its diagnosis is usually based to symptoms and apparent disease patterns. MRI scans show distinct lesions in brain and spinal cord of MS patients. FTY720 (Fingolimod), is an immunomodulator which is highly effective in animal model systems for transplantation and autoimmunity (11). It is the first in a new class of drugs called sphingosine-1-phosphate receptor (S1PR) modulators (12) and first oral drug to be approved by the US Food and Drug Administration (FDA) for MS treatment. Its structure is derived from myriocin (also known as ISP-1), which is a chemical metabolite of the fungus *Isaria sinclairii* (13). FTY720 is structurally analogous to sphingosine (9) (Figure 1:2).

Similar to sphingosine, FTY720 is also phosphorylated by Sphingosine kinase 2 (14). However, FTY720 is not phosphorylated by sphingosine kinase 1 and is believed to

bind only to four of the five GCPRs ($S1P_1$, $S1P_3$, $S1P_4$, and $S1P_5$) (15). This immune modulator has the highest binding affinity to $S1PR_1$ and a relatively lower affinity to $S1PR_{3-5}$; but none to $S1PR_2$. The biologically active form of FTY720 is found to be the (s)-enantiomer (16). The phenyl ring between its polar head and the lipophilic tail has shown to increase the agonism at $S1PR_5$, loss of activity in $S1PR_2$ and loss of stereo-specificity at $S1PR_{1,3}$ (17). The lipophilic tail of FTY720 is important for binding to the hydrophobic pocket of these receptors.

In a pharmacokinetics study (18), FTY720 is found in blood when administered intravenously; but not FTY720-P. However, a higher level of FTY720-P was found in blood when administered orally. Since it is known that sphingosine kinase 2 is highly expressed in the liver, this suggests that the first-pass metabolism generates FTY720-P (18). Eventually, FTY720 gets metabolized in the liver by cytochrome P450 CYP4F enzyme with a half-life of 5-6 days (19).

Although the phosphorylated FTY720 is an agonist to the S1P receptors, it induces internalization and degradation of the S1P receptor (4). This interferes with the normal egress of the lymphocytes thus inducing a prolonged state of immunosuppression. It takes about 2 to 8 days for full recovery to the normal expression levels of the $S1P_{1, 3-5}$ receptors. As a result, the FTY720's activity, caused by short term exposure, leads to a prolonged immunosuppressant action.

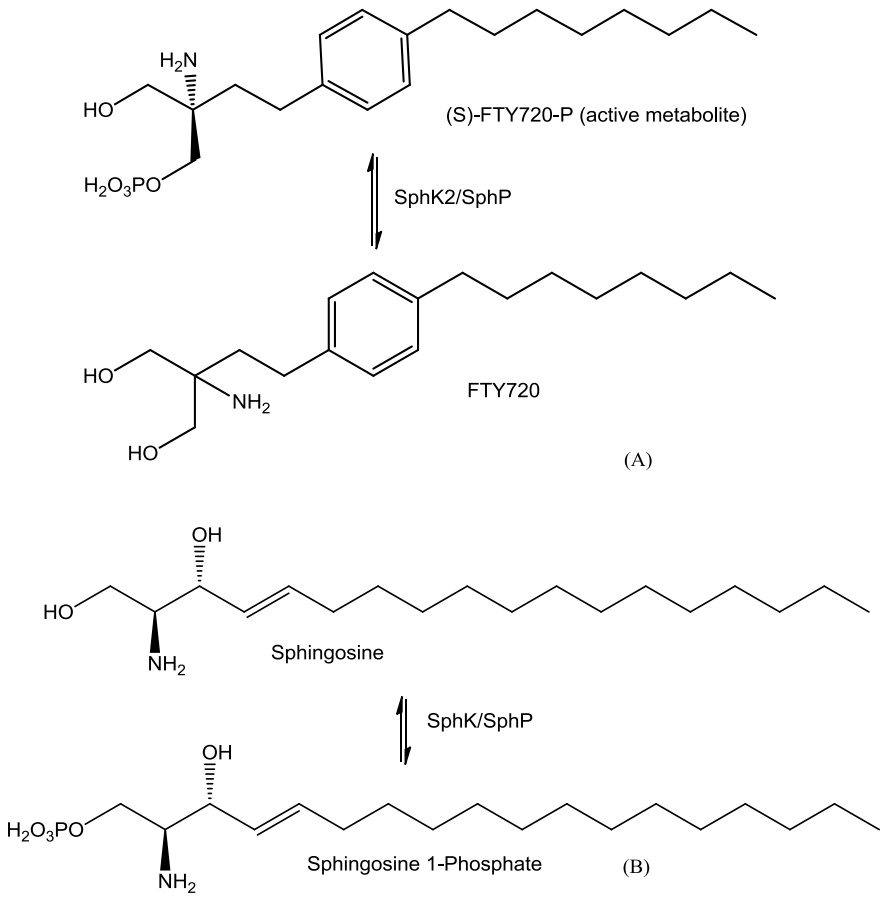

Figure 1:2 Chemical structures of FTY720 analog (A) and sphingosine (B). The phosphorylation of sphingosine is catalyzed by SphK1 and SphK2 to yield S1P. In contrast, FTY720 is phosphorylated only by SphK2 to produce FTY720-P. Such phosphorylation processes is reversible with the help of SphP for both immune suppressors.

1.4 Bodipy-FTY720 and Thesis Outline

To study the action mechanism of this novel immunosuppressor at the single-cell level, we used a newly synthesized Bodipy-labeled FTY720 analogs (namely, LZ 532C and LZ570). Bodipy (4,4-difluoro-4-bora-3a,4a-diaza-s-indacene) is relatively hydrophobic fluorophore with a large extinction coefficient and fluorescence quantum yield (20) (21) (22) (23), which make it ideal for fluorescence-based studies. In these Bodipy-FTY720 derivatives (Figure 1:3), the Bodipy fluorophore is connected via the alkyl side chain in

order to retain the hydrophilic head group of FTY720. The two analogs are generous gifts from our collaborator, Dr. Robert Bittman, Queen's College, NY (24).

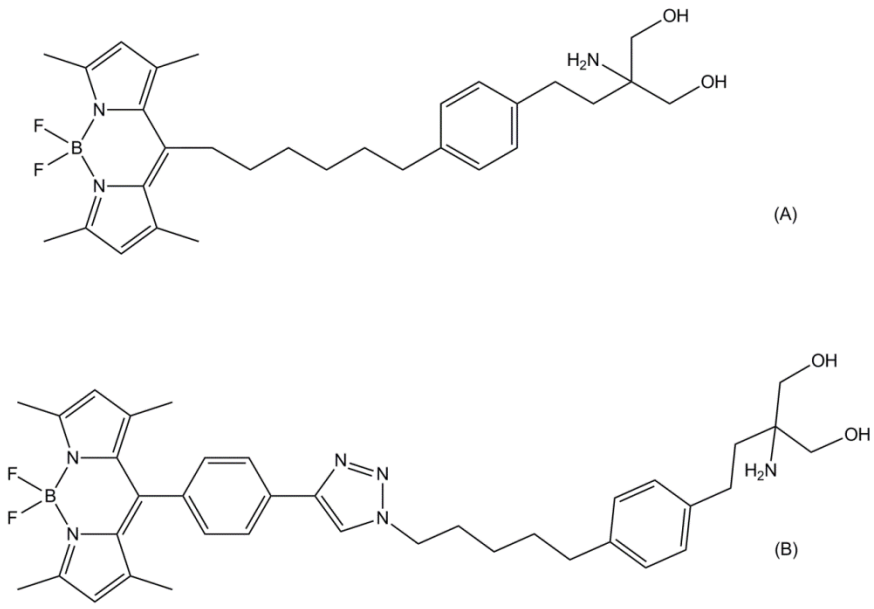

Figure 1:3 Chemical structures of the two fluorescently tagged derivatives of FTY720 (i.e., Bodipy-FTY720) used in these studies. In both derivatives (A: LZ570; B: LZ532C), the Bodipy moiety is separated from the phosphorylation site of FTY720, which key for Bodipy-FTY720-P binding with the S1P receptors.

Our working hypothesis (Figure 1:4) in this project is that the Bodipy-FTY720 derivatives (LZ532C and LZ570) will be phosphorylated by sphingosine kinase 2 (SphK2) prior to binding to sphingosine-1-phosphate receptor 1 ($S1PR_1$) followed by internalization and degradation of the receptor. In another word, the fluorescent Bodipy-FTY720 would behave the same way as the parent FTY720 and with negligible effect by the Bodipy moiety on related associations with cellular organelles. In addition, such comparative studies would enable us to examine how the linker between Bodipy moiety and phosphorylation site in these two FTY720 derivatives may affect the cellular uptake and associations of Bodipy-FTY720. The research outlined in this thesis is designed to

test this hypothesis in adherent mouse embryo fibroblast C3H10T1/2 cells. Chapter 2 describes the materials and methods used in this project. Our results and discussion section is outlined in Chapter 3 followed by the conclusions and future outlook in Chapter 4. Protocols used in these studies are also included as Appendices.

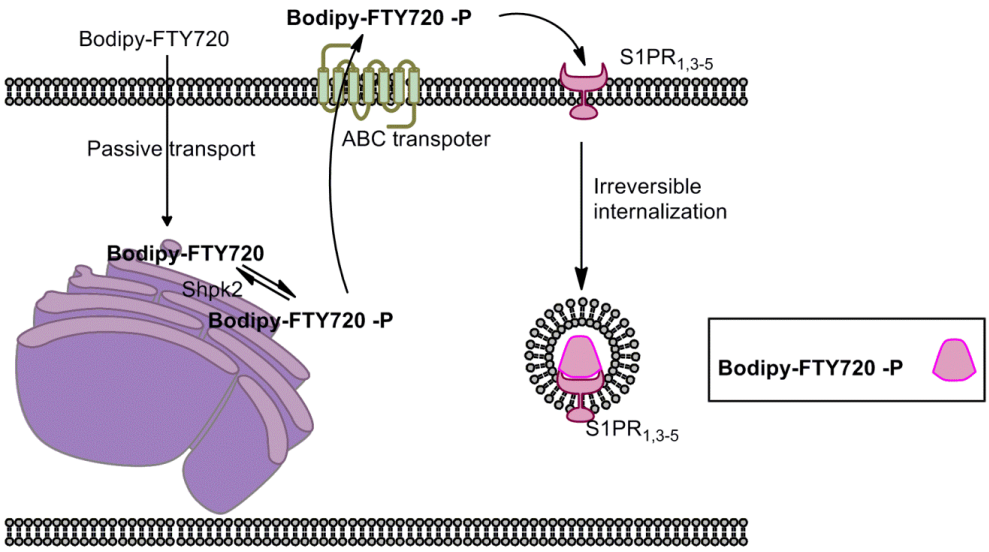

Figure 1:4 Schematic description of the underlying working hypothesis of this project. Following its cellular uptake, Bodipy-FTY720 will be localized in the ER, where it will be phosphorylated by SphK2. In return, the Bodipy-FTY720-P is secreted through ABC transporter to the extracellular milieu prior to its binding to S1PRs, internalization, and the ultimate degradation.

Chapter 2. Materials & Methods

2.1 Chemicals

2.1.1 Bodipy-FTY720

The synthesis of Bodipy-FTY720 was described previously (24) and the chemical structure of two analogs (LZ532c and LZ570) is shown in Figure 1:3. Stock solution of FTY720 was prepared in ethanol (1 mg/mL) and stored at 4°C. The steady-state absorption (maximum λ_{abs} = 500 nm) and emission (maximum λ_{fl} = 508 nm) spectra of Bodipy-FTY720 derivative (LZ532c) are shown in Figure 2:1. They were measured in ethanol (ε = 72000 $M^{-1}cm^{-1}$) at 25°C.

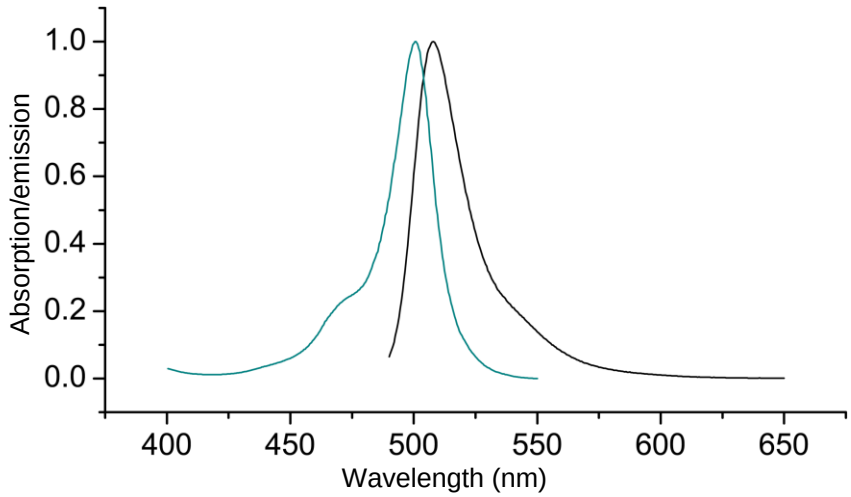

Figure 2:1 Steady state spectroscopy of LZ532C (6.3 μM in ethanol), a fluorescent analog of FTY720. The maximum absorption and emission wavelength of LZ532C is 500 nm and 508 nm, respectively at 25°C. The corresponding maximum extinction coefficient at 500 nm is ε=72000 $M^{-1}cm^{-1}$. Similar spectra were observed for LZ570 under the same conditions with a negligible spectral shift.

The absorption spectrum of Bodipy-FTY720 was recorded at a concentration of ~6.3 μM using Beckman spectrophotometer (DU800). The corresponding emission spectrum was recorded at a concentration of 0.63 μM using Fluorolog spectrofluorimeter (FL1000). Similar absorption and emission spectra were observed for LZ570 derivative in the same solvent with negligible spectral shift.

2.1.2 Rhodamine Green

A photostable fluorophore, Rhodamine green (Invitrogen), was used to as a reference for calibrating our experimental FCS and time-resolved fluorescence anisotropy systems. Diluted solutions of 1 μM and 1 nM concentrations were prepared in Phosphate Buffered Saline (PBS, pH 7.4, GIBCO) for time-resolved fluorescence anisotropy and fluorescence correlation spectroscopy measurements, respectively.

2.1.3 ER Tracker Red

ER Tracker Red™ Dye (Molecular Probes) was used to label the endoplasmic reticulum in C3H 10T1/2 cells for co-localization studies. A stock solution (1 μM) was prepared in DMSO and aliquoted before being frozen with desiccant for storage as recommended by the supplier.

2.2 Cell Culture and Staining

2.2.1 Cell Culture

The adherent mouse embryo fibroblast (C3H 10T1/2, CCL-226™) cells and their recommended culture media were purchased from American Type Culture Collection (ATCC). This cell line has been used previously as model system for S1P studies (25). The cells were grown in Eagle's Basal Medium (BME) Media containing 2 mM L-

glutamine supplemented with 10% heat inactivated Fetal Bovine Serum (FBS), 7.5% w/v% Sodium Bicarbonate and Penicillin (100U/ mL medium)-Streptomycin (100 mg/ mL medium). Cells were cultured in T-75 flasks (BD Bioscience) in a 37°C incubator with 5% CO_2 and allowed to reach 70-90% confluence before passing. For long term preservation, cells were frozen in standard media with 5% DMSO in liquid nitrogen. For imaging experiments, cells were plated at 100,000 – 120,000 cells/mL in glass-bottom Petri dishes (MatTek) and incubated overnight before measurements.

2.2.2 Staining

Bodipy-FTY720 was added to the cell culture media and was incubated for 10 mins before washing three times with Tyrode's (135 mM NaCl, 5 mM KCl, 1mM $MgCl_2$, 1.8 mM $CaCl_2$, 20 mM HEPES, and 5 mM glucose) buffer. A volume of 2 mL of the above buffer was used to replace the culture media while carrying out the experiment. Staining concentrations of Bodipy-FTY720 are 2 μM for imaging and time resolved anisotropy studies as compared with 20 nM for single-molecule fluorescence autocorrelation studies. Overnight collections of media samples were done at 3 μM of Bodipy-FTY720 where the staining procedure remained the same.

2.3 Methods

2.3.1 DIC and Confocal Imaging

The experimental setup used for confocal and differential interference conference (DIC) imaging of labeled cells consists of an Argon ion laser system (488 nm), an inverted microscope (IX81 Olympus) with a 1.2NA/60X water immersion microscope objective (Olympus) and the laser scanning unit (FV300, Olympus). The epifluorescence of the

Bodipy-FTY720-labeled cells was filtered using both an HQ525/30 M and FITC/GFP filter set (LZ532C). For ER-labeled cells, we used TRITC/TXRED filter set. Image acquisition and processing were carried out using the FlowView software. The applications MetaMorph or Image J were also used for additional image processing.

2.3.2 Fluorescence Lifetime and Anisotropy Measurements

The experimental set up (Figure 2:2) used for fluorescence lifetime and polarization anisotropy measurements has been described elsewhere in detail (26). The confocal system described above was modified to accommodate two-photon (2P) fluorescence lifetime imaging (FLIM) and polarization imaging of Bodipy-FTY720-labeled cells using 950 nm femtosecond laser pulses, which are generated by a titanium-sapphire laser system (Mira 900-F, Coherent, Santa Clara, CA). The second harmonic (475 nm) was used for complementary one-photon (1P) excitation experiments at a reduced repetition rate (4.2 MHz, Mira 9200, Coherent). The epifluorescence signal was directed toward two microchannel plate photomultiplier tubes, MCP-PMT, (R3809U, Hamamatsu, Hamamatsu City, Japan) through two Glan-Thompson polarizers using a 50/50 beam splitter. A histogram of fluorescence photon arrival times (i.e., a fluorescence decay) was recorded using a SPC 830 module (Becker and Hickl, Berlin, Germany) (19).

A 525/50 nm bandpass emission filter was used for single-point, 1P-fluorescence lifetime and anisotropy measurements of Bodipy-FTY720, either in cells or secreted in culture medium. For 2P-fluorescence imaging of Bodipy-FTY720, an additional 690 nm short pass filter was also used (along with a 525/50 BP filter) to further suppress any infrared laser scattering.

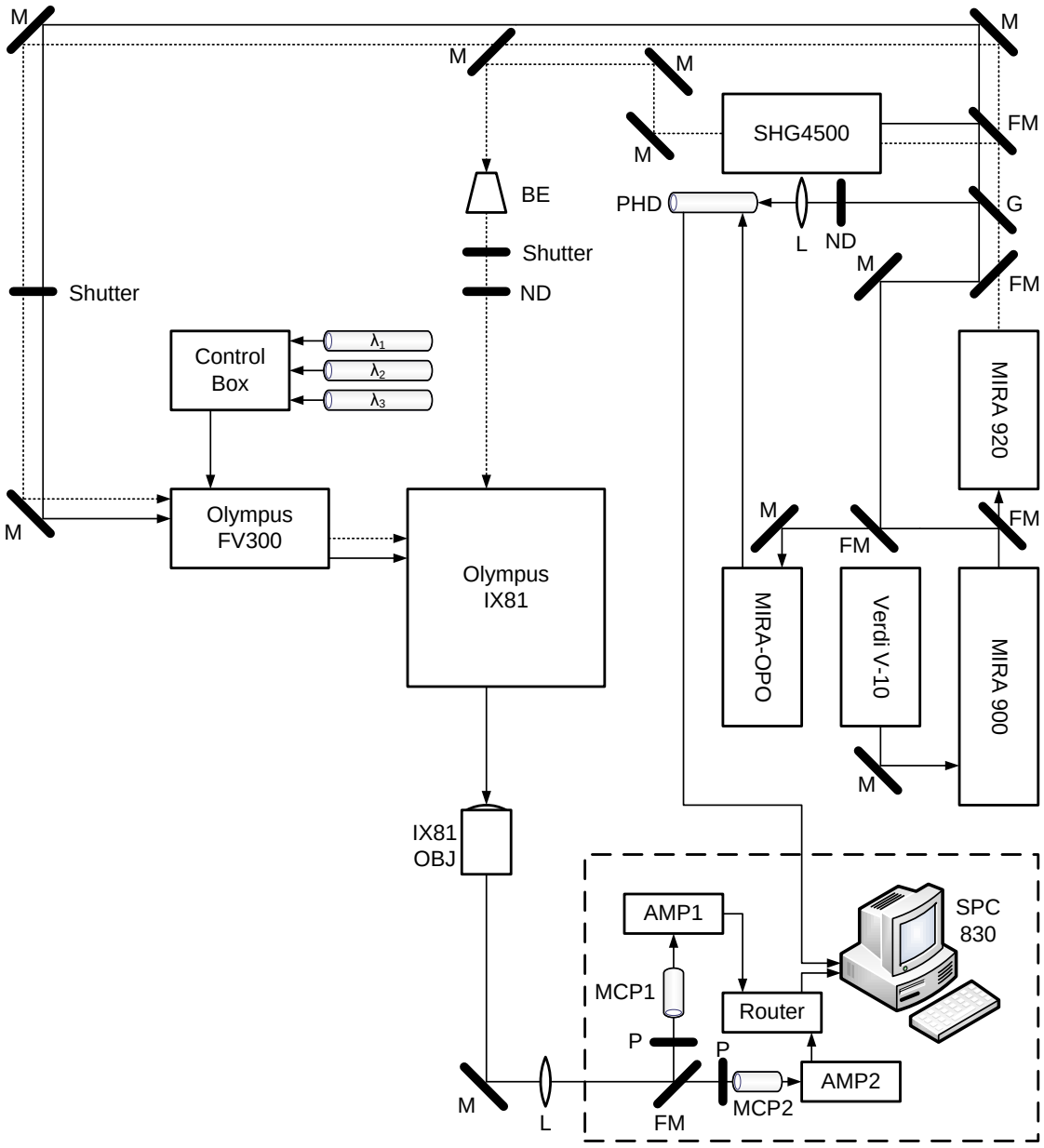

Figure 2:2 Schematic diagram of the confocal and two-photon microscopy system, equipped with two-photon fluorescence lifetime imaging (FLIM) capabilities. The laser scanning confocal microscopy consists of fiber-coupled lasers (cw: 435, 488, 514, 550, and 625 nm), scanning unit (FV300, Olympus), and an inverted IX81 microscope with 1.2NA/WI objective. A complete femtosecond laser system (Verdi V-10, MIRA 900: 120 fs, 76 MHz), pulse picker, a second harmonic generation, and a home-built detection unit are used for FLIM and anisotropy studies. This laser system is designed of generating a wavelength ranging from 350 – 1000 nm and beyond for a wide range of biomolecular studies.

2.3.3 Time Resolved Fluorescence

Based on the fluorophore's chemical structure and its local environment, the fluorescence intensity decay ($I_{54.7}$), detected at magic-angle polarization (54.7°) of a chromophore is generally described as:

Equation 2.1

$$I_{54.7}(t,x,y) = \sum_{i=1}^{2} \alpha_i(x,y) \cdot e^{-t/\tau_i(x,y)}$$

The time constants (τ_i) and amplitudes (α_i) were used to calculate the average fluorescence lifetime,

Equation 2.2

$$\langle \tau_{fl} \rangle = \frac{\sum_{i=1}^{2} \alpha_i \tau_i}{\sum \alpha_i}$$

We used two operational modes of time-correlated single-photon counting (TCSPC): one with 2P laser scanning (i.e., 2P-FLIM) and another where the 1P excitation laser was strategically focused (area of ~0.7 μm^2) on a selected area (*i.e.*, single-point measurements). In 2P-FLIM, 256 pixels × 256 pixels were used with 256 time bins per pixel. The complementary single-point measurements provided higher temporal resolution (1024 time bins). A non-linear least-square fitting routine (SPCImage, Becker & Hickl) was used to analyze fluorescence decays, deconvoluted from the system response function (full width half maximum ~50 ps). The residual and reduced χ^2-value (1.0-1.3) were used to assess the goodness of the fit.

2.3.4 Time Resolved Anisotropy

Time-resolved anisotropy allows for probing the hydrodynamic volume of a tumbling fluorophore during its excited-state lifetime as well as the restriction imposed by its local environment. For time-resolved anisotropy, the resulting epifluorescence of the samples was collected using T-format method (Figure 2:2), where the intensities of parallel and perpendicular components are measured simultaneously using two MCP-PMT detectors (27). The fluorescence signal was filtered using the R488 dichroic mirror and the HQ525/30 filter (Semrock) and polarization-analyzed using Glan-Thompson polarizer. The time correlated single photon counting histogram was then recorded using SPC830 module (Becker and Hickl) and a maximum photon counts ranged between 60 - 65 kHz for enhanced signal-to-noise ratio. Tail-matching method (27) was used to calculate the G-factor of our experimental setup using rhodamine green (1 μM, Invitrogen) as a control before every anisotropy measurement.

At a given local inside a living cell, the fluorescence anisotropy *r(t,x,y)*, can be calculated using two simultaneously measured fluorescence intensity of parallel $I_{\parallel}(t,x.y)$ and perpendicular $I_{\perp}(t,x,y)$ polarization, at a given pixel (x,y), with respect to the polarization of excitation laser by (28);

Equation 2.3

$$r(t,x,y) = \frac{[I_{\parallel}(t,x,y) - G.I_{\perp}(t,x,y)]}{[I_{\parallel}(t,x,y) + 2.G.I_{\perp}(t,x,y)]}$$

where the G factor accounts for a potential bias of polarized-fluorescence detection. For one photon steady state anisotropy, G factor is calculated using a small fluorophore with

much faster rotational time as compared with its fluorescence lifetime (*e.g.* rhodamine green) with tail matching approach.

Depending on the molecular heterogeneity and surrounding local environment, time resolved anisotropy decay is generally described as;

Equation 2.4

$$r(t,x,y) = \sum_{i=1}^{3} \beta_i(x,y) \cdot e^{-t/\varphi_i(x,y)}$$

where φ is the rotational time and the sum of pre-exponential factors (β_i) is equal to initial anisotropy (r_0). A fluorophore bound to a large molecule may undergo segmental motion on a fast time scale while the overall rotational time (φ_i) of the combination would be slower with respect to the fluorescence lifetime of the fluorophore. To quantify the degree of order among fluorophores in biomembrane, the order parameter (S) is calculated from the time-resolved anisotropy and is given by;

Equation 2.5

$$S = \sqrt{\frac{\beta_{slow}}{r_0}}$$

The initial anisotropy depends on the orientation angle (δ) between absorbing and emitting dipoles such that (29);

Equation 2.6

$$r_0(x,y) = \frac{2\gamma}{2\gamma+3}\left[\frac{3\cos^2\delta(x,y)-1}{2}\right]$$

Where, γ is the number of excited photons (γ = 1 for 1P and γ = 2 for 2P) and maximum theoretical value of r_0 is 0.4 for 1P and 0.57 for 2P.

The time resolved fluorescence anisotropy of an ensemble of non-interactive fluorophores with different excited-state lifetimes and hydrodynamic volumes is given by associated anisotropy and it is defined as (30);

Equation 2.7

$$r(t) = \frac{\sum_i^m \alpha_i \cdot e^{-t/\tau_i} \cdot \beta_i \cdot e^{-t/\varphi_i}}{\sum_i^m \alpha_i \cdot e^{-t/\tau_i}}$$

The rotational diffusion time (φ) of a spherical molecule in a given pixel (x,y), depends on the hydrodynamic volume (*V*) and the viscosity (η) (27) and is given by;

Equation 2.8

$$\varphi_i(x,y) = \frac{\eta_i(x,y).V(x,y)}{RT}$$

Where *T* is the temperature, *R* is the universal gas constant. When it is difficult to independently address whether a molecule stays monomeric in a cellular environment with unknown local viscosity, it is appropriate to discuss the *apparent hydrodynamic volume* (V_{app}) where;

Equation 2.9

$$V_{app}(x,y) = \frac{\eta_i(x,y).V(x,y)}{\eta_w(x,y)}$$

The data were finally analyzed using Origin 8.1 software.

2.3.5 Fluorescence Correlation Spectroscopy

Multimodal fluorescence correlation spectroscopy (FCS) was used to study translational diffusion of single molecules (10^{-11} – 10^{-9} M) as they diffuse through an open observation volume (~10^{-15} L). In our home-built FCS setup (Figure 2:3), which is described in details elsewhere (31), the sample is excited using a fiber-coupled CW laser (488 nm) and the

epifluorescence is isolated from the excitation light using a dichroic mirror with HQ525/30 M filter (Semrock) for Bodipy-FTY720 emission. The fluorescence fluctuation signal is then focused on an optical fiber (50 µm in diameter), which acts as a confocal pinhole prior to reject out-of-focus fluorescence photons, prior to detection by an avalanche photodiode (APD, SPCM CD-2969, Perkin-Elmer, Fremont, CA). The time-dependent fluorescence fluctuations are then autocorrelated using an external multiple-tau-digital correlator (ALV/6010-160, Langen/Hessen, Germany). The system is routinely calibrated using a photostable fluorophore, rhodamine green (1 nM, Invitrogen), with a known translational diffusion coefficient (D_T ~2.8x10^{-6} cm^2/s).

The continuous wave (CW) laser system was controlled using MetaMorph software and the intensity was kept at a maximum 17% - 19% from the software (50% at the 488 nm laser head). The data obtained was analyzed using Origin 8.1 (Origin®, Northampton, MA, USA).

The autocorrelation function, $G(\tau)$, of fluorescence fluctuation, $\delta F(t)$, is defined as,

Equation 2.10

$$G(\tau) = \frac{[\delta F(t).\,\delta F(t+\tau)]}{\langle F(t)\rangle^2}$$

where F(t) is the time-dependent fluorescence intensity at a time t. The autocorrelation for a single diffusing species in three-dimension observation volume is given by;

Equation 2.11

$$G_D(\tau,x,y) = \frac{1}{N}\frac{1}{\left[1+{}^{\tau}/_{\tau_D(x,y)}\right]\left[\sqrt{1+{}^{\tau}/_{\omega_0{}^2\tau_D(x,y)}}\right]} + c$$

Where N is the number of molecules with a diffusion time τ_D and a structure parameter is the axial-to-lateral extension ($\omega_o = z/\omega_{xy}$) of the observation volume. Stokes-Einstein model states that the diffusion coefficient (D_T) of a spherical molecule in a homogeneous solvent, $D_T = \omega_{xy}^2/4\tau_D = k_B T/6\pi\eta a$, depends on Boltzmann constant (k_B), the hydrodynamic radius (a) of the diffusing species, and the viscosity (η) of the local environment. The baseline correction (c) accounts for any potential scattered light, which does not correlate. In case of two diffusing species, the resulting autocorrelation function that describes the corresponding fluorescence fluctuation is given by:

Equation 2.12

$$G(\tau,x,y) = \frac{1}{N}\left(f\frac{1}{1+{\tau}/{\tau_1}}\frac{1}{\sqrt{1+{\tau}/{{\omega_0}^2\tau_1(x,y)}}} + (1-f)\frac{1}{1+{\tau}/{\tau_2}}\frac{1}{\sqrt{1+{\tau}/{{\omega_0}^2\tau_2(x,y)}}}\right) + c$$

Where τ_1 and τ_2 are the diffusion times of the two diffusion species and *f* is the population fraction of the first species as compared with (*1-f*) for the second one.

In contrast, when the fluorophore undergoes anomalous (i.e., non-Brownian) diffusion (*e.g.* in a biomembrane), the following equation is used to describe the corresponding fluorescence fluctuation autocorrelation:

Equation 2.13

$$G(\tau) = \frac{1}{N}\left(\frac{1}{1+\left({\tau}/{\tau_1}\right)^{\alpha}}\right) + c$$

Where α denotes the degree of deviation from Brownian diffusion; α=1 for Brownian diffusion and α<1 for anomalous diffusion (32).

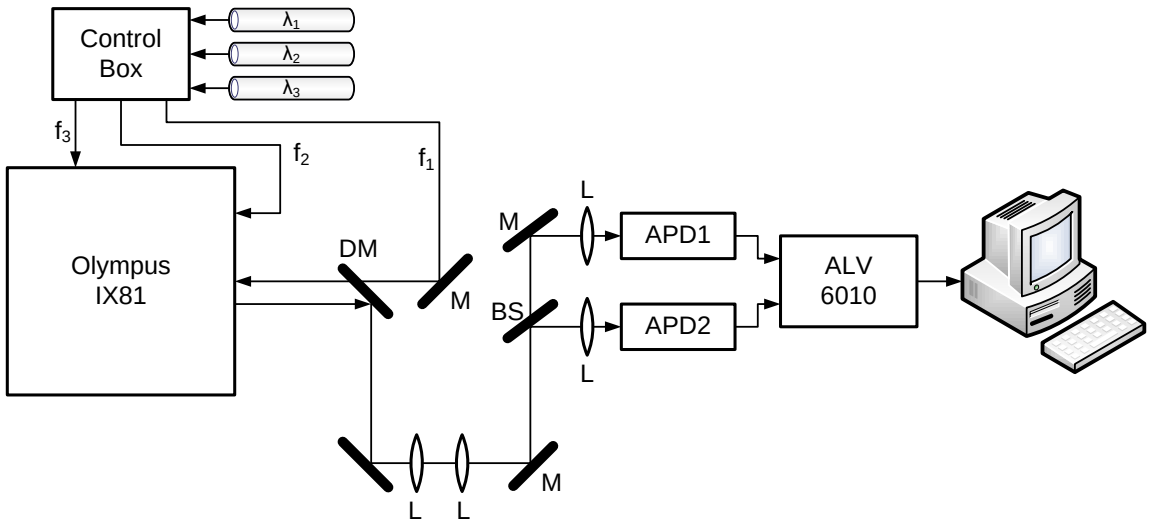

Figure 2:3 A sketch of the experimental setup used for wide field, total internal reflection (TIRF) and fluorescence correlation spectroscopy (FCS). The system consists of a fiber-coupled laser (488, 561, 654 nm) system (with AOTF control unit), inverted microscope (IX81, Olympus), two fiber-coupled avalanche photodiodes (APDs) and a multiple-tau-digital correlator (ALV 6010). Fiber 1 (f_1) is connected to the FCS system, f_2 is connected to the TIRF port and f_3 is connected to the wide field. M: mirror, BS: beam splitter, DM: dichroic mirror and L: lens.

Chapter 3. Results and Discussion

3.1 Cellular Uptake and Distribution of Bodipy-FTY720 in C3H10T1/2 Cells

3.1.1 Confocal and DIC Imaging of Bodipy-FTY720 in C3H10T1/2 Cells

To examine the effect of Bodipy moiety on the uptake and partitioning of Bodipy-FTY720 in mouse fibroblast C3H10T1/2 cells (14), we carried out time-lapse imaging using confocal and DIC microscopy. Figure 3:1 exhibits representative confocal (A) and DIC (B) images of C3H10T1/2 cells following 10-minutes incubation with 2 μM of Bodipy-FTY720 in the 2 mL culture media. Within the context of cell morphology (Figure 3:1, B), the low-zoom confocal image in (Figure 3:1, A) displays an affinity of Bodipy-FTY720 to the cytoplasm of C3H10T1/2 cells with a negligible presence in the nucleus. Figure 3:1(C) shows a high-resolution image of Bodipy-FTY720-labeled cells at the cell-coverslip interface using 1.4NA, oil-immersion objective and TIRF configuration. Both the confocal (Figure 1:1, A) and TIRF (Figure 3:1, C) images reveal encapsulation of the Bodipy-FTY720 and vesicle formation inside the C3H10T1/2 cell, which would likely undergo exocytosis at a later stage.

Based on time-lapse imaging (see below), these vesicles are mobile and are currently being investigated to quantify their sizes and diffusion patterns using single-particle tracking approach. These observations represent the first indication that the Bodipy-FTY720 is likely to be phosphorylated, associated with the S1P receptors, and internalized with the S1P receptors; just as the parent FTY720.

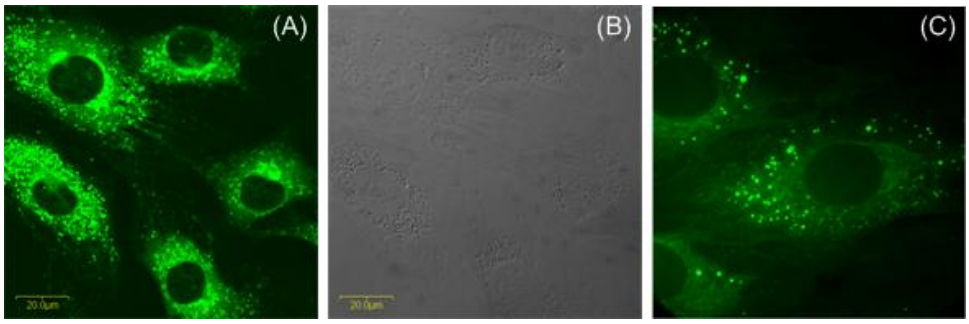

Figure 3:1 Confocal and DIC images reveal the distribution and vesicle formation of Bodipy-FTY720 in living C3H10T1/2 cells. Confocal (A) and DIC (B) images reveal the distribution of Bodipy-FTY720 (LZ532C) within the context of cell morphology. The vesicle formation (encapsulation of a likely Bodipy-FTY720-P complexed with S1P receptors) is time dependent with respect to staining (see below Figure 3:2). A representative TIRF image (C) of labeled cells also reveals Bodipy-FTY720 (LZ532C) distribution and vesicle formation near the cell-coverslip interface (~100 nm thick region) with suppressed background signal using 1.4 NA, oil-immersion microscope objective.

3.1.2 Time-Lapse Imaging of Bodipy-FTY720 Uptake by C3H10T1/2 Cells

To examine the time-dependence of internal vesicle formation, time-lapse confocal imaging was carried out as a function of incubation time with Bodipy-FTY720. Time-lapse imaging series (both confocal and DIC) was recorded using on-stage incubation (where 0.5 μM of Bodipy-FTY720 was added at time zero) over a 60-minute period. Figure 3:2 exhibits representative frames (1 minute/frame) from these time-lapse images. Under these incubation conditions, image processing of this time-lapse imaging indicates 6±1 minutes for 50% concentration of Bodipy-FTY720 inside the cells prior to reaching a plateau (*i.e.*, saturation) after ~20 minutes.

At saturation, the cellular uptake becomes heterogeneous with an apparent high concentration near the nucleus. At early stages of incubation, we argue that Bodipy-FTY720 is transported through the plasma membrane (via passive diffusion *for example*)

prior to phosphorylation by SphK2, which is likely to occur in the endoplasmic reticulum (ER). At the zero-time (Figure 3:2, A), the fluorescence signal of Bodipy-FTY720 in the culture media is negligible due to the low concentration (0.5 μM) and perhaps its hydrophobic nature in the culture medium. Such observation also indicates the sensitivity of Bodipy-FTY720 fluorescence to its local environment.

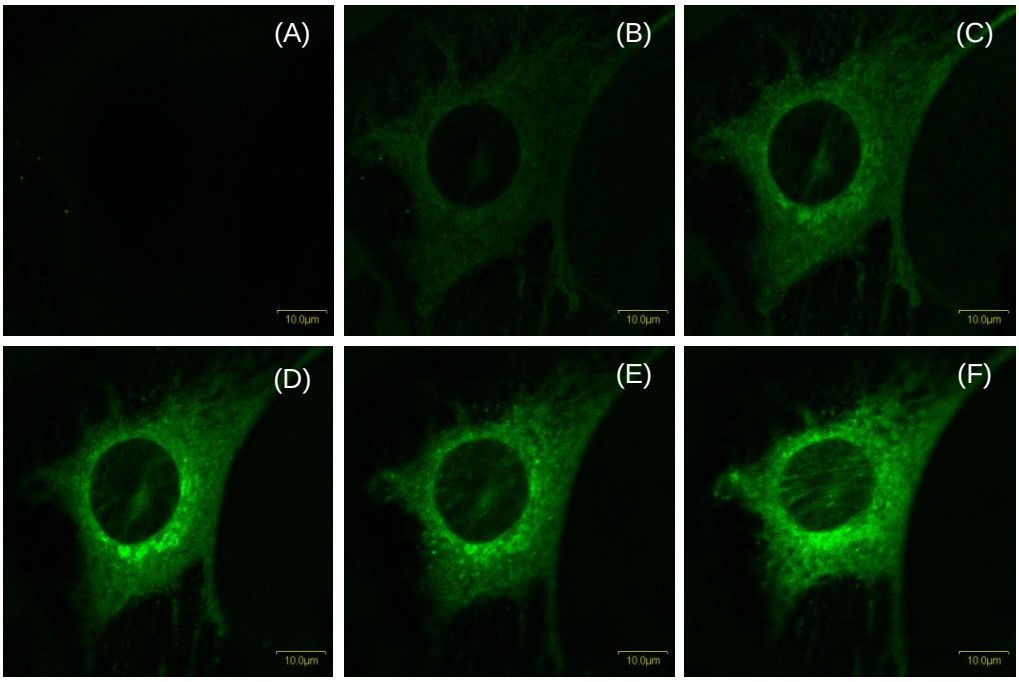

Figure 3:2 Representative frames from time-lapse confocal images of Bodipy-FTY720 in cultured C3H10T1/2 cells. The cells were stained on the microscope stage at time-zero followed by time dependent confocal and DIC (not shown) imaging over 60 minutes period. These representative confocal images were recorded at 0 min (A), 2 min (B), 5 min (C), 15 min (D), 30 min (E), 60 min (F) after labeling the cells on the stage at room temperature. The images were recorded with 1.2 NA, water-immersion microscope objective.

Below, we use a multi-labeling scheme to examine whether Bodipy-FTY720 resides in the ER membranes.

3.1.3 Bodipy-FTY720 Resides in the ER of C3H10T1/2 Cells

To examine whether Bodipy-FTY720 resides in the endoplasmic reticulum, C3H10T1/2 cells were doubly stained with Bodipy-FTY720 (1 μM) and Glibenclamide-Bodipy-FL (2 μM), which is known ER label. Both labeling processes underwent the same incubation time (15 minutes). These images were recorded using 488-nm laser (Bodipy-FTY720, Figure 3:3, A) and 561-nm laser (ER tracker, Figure 3:3, B).

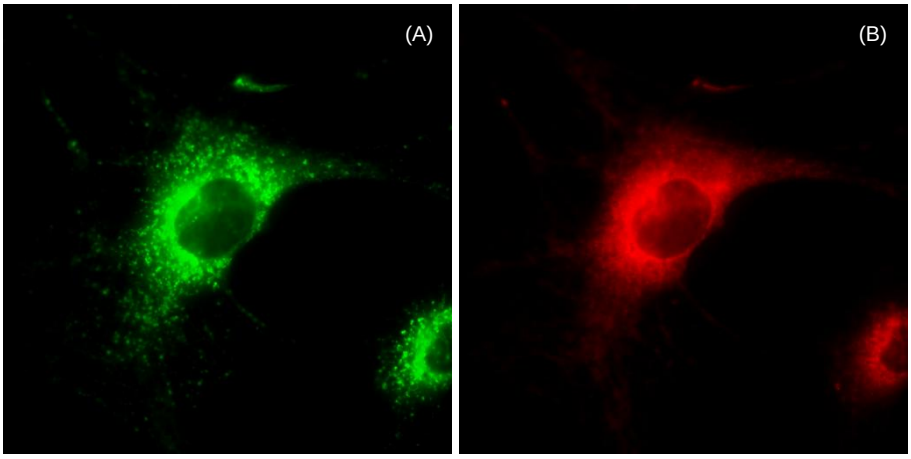

Figure 3:3 Co-localization of Bodipy-FTY720 and Glibenclamide-Bodipy-FL (an ER tracker-red). The images were taken after staining the cultured C3H10T1/2 cells with both LZ570 (A) and Glibenclamide-Bodipy-FL (B) using 488 nm and 561 nm, respectively. The green-red correlation plot of these images is shown in (Figure 3:4).

Representative two-channel images are shown in the Figure 3:3, which indicate co-localization of the two dyes as revealed by the correlation plot (Figure 3:4). As a result, we conclude that Bodipy-FTY720 resides in the ER of C3H10T1/2 cells following its transport through the plasma membrane.

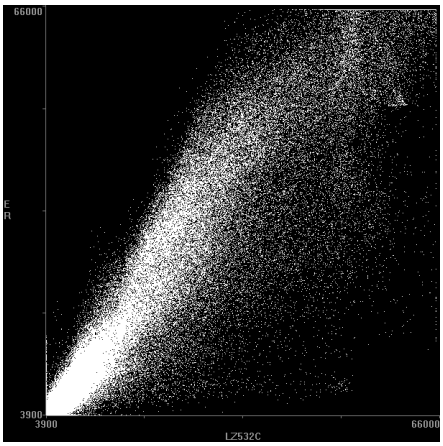

Figure 3:4 Correlation Plot of the doubly-labeled C3H10T1/2 cells with ER tracker-red label and Bodipy-FTY720 of Figure 3:3 (correlation = 0.941)

3.2 Environmental and Structural Heterogeneity of Bodipy-FTY720 in C3H10T1/2 Cells

Fluorescence lifetime of a given fluorophore is sensitive to both its chemical structure and surrounding environment. This is in contrast with conventional intensity imaging, where fluorescence intensity depends on the fluorophore's concentration. To examine the local environment and structural heterogeneity of the intracellular Bodipy-FTY720, we used two-photon fluorescence lifetime imaging microscopy (see Methods) on labeled, adherent C3H10T1/2 cells. The cells were incubated at 37°C for 4 hours after labeling them with Bodipy-FTY720, and were taken out for FLIM imaging after replacing the culture media with tryrode's buffer. The average lifetime of Bodipy-FTY720 was 3.9±0.3 ns, which does not reflect the observed heterogeneity based on pixel-to-pixel analysis. For example, the fluorescence lifetime near the nucleus is ~4.5 ns, whereas ~3.5 ns lifetime was measured away from the nucleus and towards the plasma membrane. Such

spatial heterogeneity suggests that the fluorescence lifetime of Bodipy-FTY720 in the ER is longer than that in the apparent vesicles.

The shorter fluorescence lifetime of Bodipy-FTY720 observed in vesicles is attributed to quenching (or fluorescence resonance energy transfer) between potential multiple copies of the fluorophore inside each vesicle. Another possibility is that the protein environment of Bodipy-FTY720 binding cite in S1P-receptor may cause such reduction of the fluorescence lifetime due to energy transfer to neighboring amino acids. This alternative interpretation of fluorescence lifetime reduction can be tested with the knowledge of the exact binding cite of Bodipy-FTY720-P, which is currently under investigation.

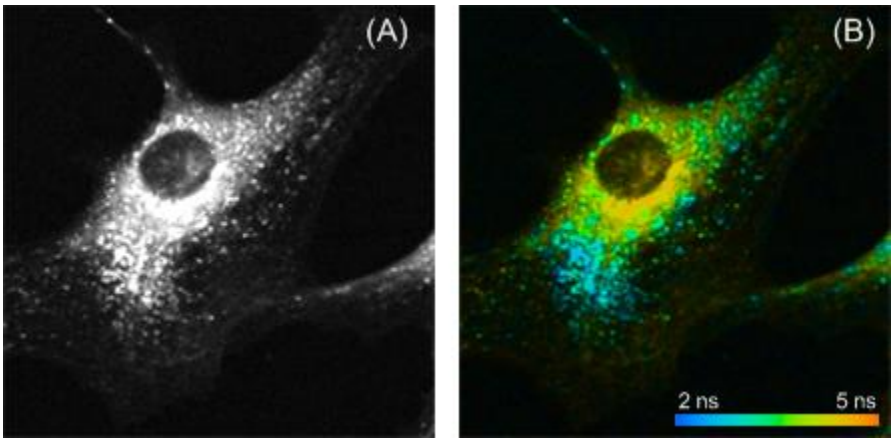

Figure 3:5 Two-photon fluorescence lifetime imaging of Bodipy-FTY720-labeled C3H10T1/2 cells. While the two-photon fluorescence intensity of (A) depends on the concentration, fluorescence lifetime in FLIM images (B) does not. These images were recorded using two-photon 950-nm excitation. [The color changes in the FLIM image show the variation of fluorescence lifetime for each pixel.] The FLIM image reveals a heterogeneous environment and structure of internalized Bodipy-FTY720 in cultured C3H10T1/2 cells. Two populations of intracellular Bodipy-FTY720 could be identified, one with a lifetime of ~4.5 ns (near the nucleus; ER) and the other ~3.5 ns (away from the nucleus, which may contains vesicles as discussed earlier). The stained cells were first imaged using confocal and DIC (not shown) microscopy before and after the corresponding FLIM image to examine potential photostress, which was negligible.

3.3 Fluidity and Order of Bodipy-FTY720 in C3H10T1/2 Cells

Single point time-resolved anisotropy measurements were carried out to examine the degree of restriction of the local environment on Bodipy-FTY720 in living C3H10T1/2 cells. The same measurements also provide insights on the order parameter of Bodipy-FTY720 in cellular environment. In these measurements, the laser was focused on randomly chosen regions in the cytoplasm and away from the nucleus. The lateral radius of the laser spot is diffraction limited (300 nm), but without the confocal restriction on the axial extension of the focal volume. Figure 3:6 exhibits a representative anisotropy decay of Bodipy-FTY720 in the ER of C3H10T1/2 cells and the fitting parameters are summarized in Table 3:1. Under the same experimental conditions, rhodamine green (PBS, pH7.4) was used as a control and for determining the G-factor. The anisotropy of free rhodamine green in a buffer decays as a single exponential with an estimated rotational time of ~120 ps and initial anisotropy of ~0.17. The smaller initial anisotropy (as compared with the theoretical value of 0.4) can be attributed to the high NA objective used in these experiments (33). The fast rotational time of rhodamine green is consistent with its hydrodynamic radius and molecular weight.

The anisotropy of cytosolic Bodipy-FTY720 decays as a biexponential (Equation 2.4) with a fast tumbling motion on the order of 1.2 ± 0.3 ns with an amplitude of β_1 = 0.052 ± 0.006. The second slow component decays on 20 ± 5 ns time scale with a relatively larger amplitude (β_2 = 0.17 ± 0.01). The observed slow rotational time of Bodipy-FTY720 is attributed to the association of this immune modulator with ER membranes in the intracellular milieu. Using these fitting parameters (Table 3:1.) of

Bodipy-FTY720 anisotropy decay, we also estimate an order parameter (*S*) of 0.88 ± 0.05, which indicate a degree of order among these fluorophores in the ER membrane.

In support with our co-localization experiment above, these results provide a direct evidence for the high affinity of Bodipy-FTY720 to ER membrane either directly or in vesicles via the S1P receptor after phosphorylation (34). It is also possible that the observation volume may include intracellular vesicles following the internalization of Bodipy-FTY720-P bound S1P receptors. Currently, we are conducting time-dependent anisotropy measurements following incubation in order to isolate rotational diffusion of Bodipy-FTY720 in the ER prior to vesicles formation.

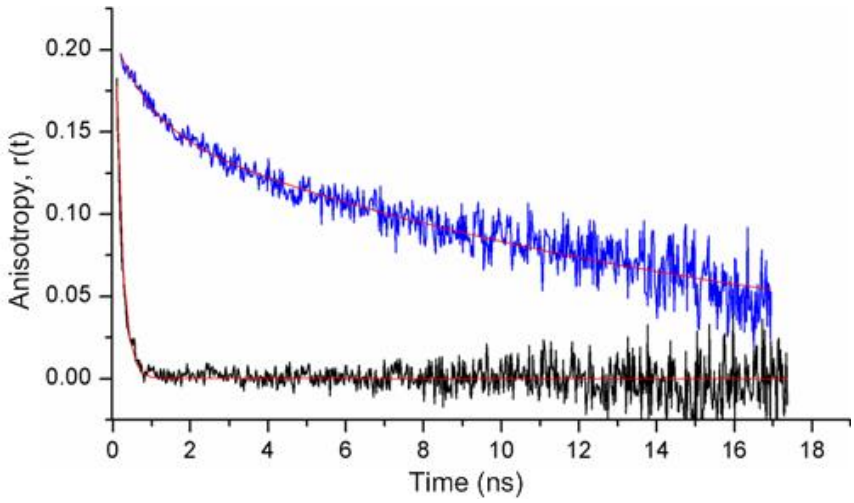

Figure 3:6 Representative anisotropy decay of intracellular Bodipy-FTY720 in C3H10T1/2 cells. The cytosolic (ER and vesicles) Bodipy-FTY720 anisotropy (curve A) decays as a biexponential with $\varphi_1 = 1.2 \pm 0.3$ ns ($\beta_1 = 0.052 \pm 0.006$) and $\varphi_2 = 20 \pm 5$ ns ($\beta_2 = 0.17 \pm 0.01$). For calibration, rhodamine green (PBS, pH7.4, 1 μM, room temperature) was measured under the same conditions. The anisotropy of rhodamine green (curve B) decays as single exponential with a rotational time (130 ± 10 ps) that was consistent with its size.

Table 3:1 Time Resolved Anisotropy of Bodipy-FTY720 in C3H10T1/2 cells follows a bi-exponential decay model (n = 5)

Cellular environment	Rotational Diffusion Model		Order Parameter (S)
	Φ_1 (β_1)	Φ_2 (β_2)	
ER membranes	1.2 ± 0.3 ns (0.052 ± 0.006)	20 ± 5 ns (0.17 ± 0.01)	0.88 ± 0.05

3.4 Translational Diffusion of Bodipy-FTY720 in the Heterogeneous Milieu of C3H10T1/2 Cells

Translational diffusion depends on the hydrodynamic radius of the diffusing species as well as the viscosity of the local environment. At the single-molecule level, FCS is the method of choice for quantifying the diffusion coefficient of Bodipy-FTY720 in the crowded cell environment, whether it is the plasma membrane or the ER of resting C3H10T1/2 cells. The same approach provides insights into whether the Bodipy-FTY720 is associated with other proteins or organelles in the living cell. As a control (Figure 3:6), the observation radius (~260 nm) in our FCS setup was calibrated using rhodamine green in PBS buffer (pH 7.4) at room temperature based on the measured diffusion time (τ_D = 0.103 ± 0.001 ms) and published diffusion coefficient (D = 2.8×10^{-8} cm^2/s). The fitting parameters are summarized in Table 3:2.

For the plasma membrane measurements, the confocal plane was adjusted manually using Z-scan to focus the laser on the upper plasma membrane and away from the coverslip (i.e., the lower membrane to avoid the substrate effect of diffusion). The regions of interest on the plasma-membrane were chosen either away from the nucleus (near the cell peripherals) or above the nucleus. At the plasma membrane, maximum fluorescence fluctuation was observed. The fluorescence fluctuation autocorrelation of

Bodipy-FTY720 in the plasma membrane of resting C3H10T1/2 cells decays as a two-dimensional anomalous diffusion (Figure 3:7, Equation 2.13) with an anomalous coefficient (α) of 0.70 ± 0.06 (n=10). The corresponding 2D-diffusion time is 25 ± 6 ms, which yields a diffusion coefficient of Bodipy-FTY720 in the plasma membrane of (11.7 ± 0.5)×10^{-9} cm^2/s (see Table 3:2. for a summary of the fitting parameters). These results indicate heterogeneity in the landscape of a restrictive plasma membrane in this cell line under resting conditions.

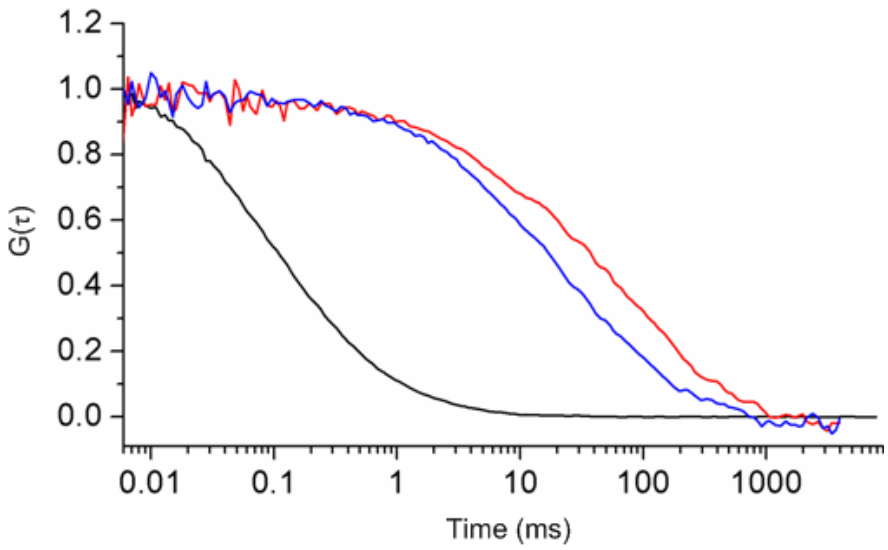

Figure 3:7 Fluorescence fluctuation autocorrelation of intracellular Bodipy-FTY720 in C3H10T1/2 cells. The fluorescence fluctuation autocorrelation of the cytosolic Bodipy-FTY720 (red curve) reveals two diffusing species with τ_{D1} = 6 ± 1 ms and τ_{D2} = 110 ± 60 ms. In contrast, the plasma membrane bound Bodipy-FTY720 autocorrelation (blue curve) indicates an anomalous diffusion with a diffusion time of τ_D = 26 ± 6 ms with α = 0.88. As a control (black curve), the fluorescence fluctuation autocorrelation of rhodamine green (PBS, pH7.4, room temperature) indicates a diffusion time of 0.08 ms under the same conditions.

In contrast with the above-mentioned diffusion in the plasma membrane, the fluorescence fluctuation autocorrelation on Bodipy-FTY720 in the cytosol is best described by a two-diffusing species model in 3D (Figure 3:6, Equation 2.12).

Importantly, one of the diffusing species in the cytosol exhibits a significantly slower diffusion coefficient as compared with that in the plasma membrane (Figure 3:7, Table 3:2). For example, 95% fraction of the Bodip-FTY720 species diffuses at a rate of (5.1 ± 0.8)×10^{-8} cm^2/s as compared with 5% of the population diffusing at a rate of (2.69 ± 0.04)× 10^{-9} cm^2/s in the cytosol of resting C3H10T1/2 cells (Table 3:2). Based on our confocal studies and time-lapse imaging, we assign the relatively fast component (5.1 ± 0.8×10^{-8} cm^2/s) to the unphosphorylated Bodipy-FTY720 in the ER membrane (35). Since the cytosolic regions of interests were chosen randomly, it is likely that some of the vesicles observed in our confocal images could be included in our observation volume. As a result, we assign the slow component (2.69 ± 0.04× 10^{-9} cm^2/s) to internalized, S1P receptor bound, encapsulated Bodipy-FTY720-P (34).

Table 3:2 Translational Diffusion of internalized Bodipy-FTY720 in C3H10T1/2 cells (n=10)

Cellular environment	Diffusion Time τ_D (ms)	Diffusion Coefficient (cm^2/s)
Cytoplasm	6 ± 1	(5.1 ± 0.8)×10^{-8}
	110 ± 60	(2.69 ± 0.04)× 10^{-9}
Plasma membrane	25 ± 6	(1.17 ± 0.5)×10^{-8}

It is worth noting that the diffusion coefficient of Bodipy-FTY720 in the plasma membrane (1.17 ± 0.5×10^{-8} cm^2/s) is about 4.3 slower than that in the ER membrane (5.1 ± 0.8×10^{-8} cm^2/s). Such distinct diffusion coefficients can be attributed to that a snapshot would likely to capture both Bodipy-FTY720 during it passive transport in the plasma membrane and Bodipy-FTY720-P associated with the S1P receptors within the observation volume (Receptor-bound Bodipy-FTY720-P on the plasma membrane would diffuse slower that membrane-bound fluorophore due to the difference in the molecular

sizes). The observed diffusion coefficient may also suggest a different structural mosaic of ER membrane as compared with the plasma membrane of resting C3H10T1/2 cells. For example, the protein-to-lipid content ratio, lipid types and cholesterol content would explain the observed difference in diffusion processes.

Using the above mentioned FCS and time-resolved anisotropy, we used the estimated translational-to-rotational diffusion coefficient ratio ($D_T / D_R = 4a^2 / 3$) to calculate the hydrodynamic radius (a) of the intracellular Bodipy-FTY720. Assuming Stokes-Einstein model, the D_T / D_R ratio is independent of the environmental viscosity surrounding the diffusing fluorophore. Our results indicate a hydrodynamic radius of ~14 nm, which is significantly larger than a free Bodip-FTY720 in a solution. In these calculations, we used the average rotational time along with the slow translational diffusion time of intracellular species.

3.5 Examining the Phosphorylation and S1P-Receptor Binding of Bodipy-FTY720

Our working hypothesis (Figure 1:4), that the transported Bodipy-FTY720 through the plasma membrane (*e.g.*, by passive diffusion) will be phosphorylated by SphK2 in the ER, secreted into the culture media via an ABC transporter, and then bind to the S1P receptors prior to internalization, encapsulation, and degradation. In another word, Bodipy-FTY720 will behave just like the parent FTY720 immune modulator, *i.e.*, negligible effect of the Bodipy moiety. Following its transport across the plasma membrane of C3H10T1/2 cells, the time-lapse imaging shows that Bodipy-FTY720 is internalized prior to encapsulation into vesicles with distinct diffusion coefficients during its association with cellular organelles.

To further test this hypothesis, we carried out time-dependent sampling (100 μL) of the cultured medium following the staining the C3H10T1/2 cells with Bodipy-FTY720 (3 μM, 2 mL of culture media). The cultured media of stained cells was sampled after 1, 2, 3, 4, 5, 24, and 48 hours from cell staining by Bodipy-FTY720. We then carried out FCS and time-resolved anisotropy measurements on the sampled cultured media to examine the size and conformational flexibility of the secreted species. The experimental systems in both measurements were calibrated using rhodamine green (PBS, pH 7.4, room temperature).

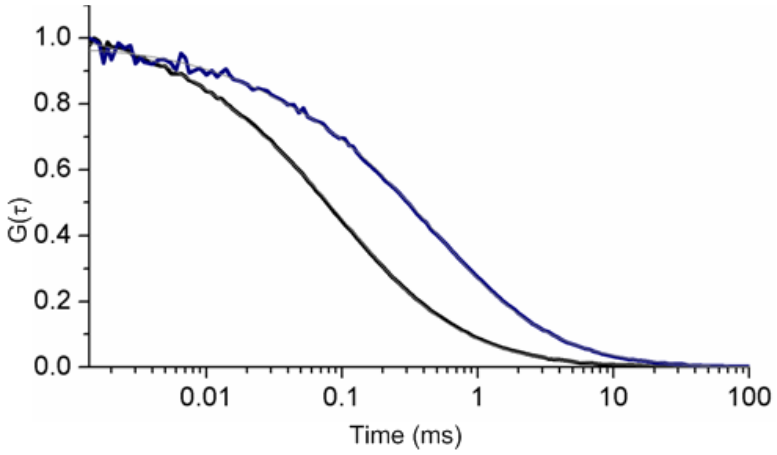

Figure 3:8 Fluorescence fluctuation autocorrelation of sampled Bodipy-FTY720 in the culture media of incubated, stained cells. The fluorescence fluctuation autocorrelation of sampled Bodipy-FTY720 in the cultured medium after 24 hr incubation indicate a diffusion time of ~0.5 ms, which is significantly slower than a free Bodipy-FTY720. Autocorrelation of rhodamine green was used for calibration with a diffusion time of τ_D = 0.08 ms (see Table 3:3 for a summary).

As a control, the diffusion time of rhodamine green under the same experimental conditions (τ_D = 0.083 ± 0.001 ms) corresponds to a diffusion coefficient of 2.8×10^{-6} cm^2/s. For further control, we examined the cultured media with and without Bodipy-FTY720 (6 nM) under the same conditions. The signal from pure culture medium was

negligible and without significant correlation amplitude. In addition, the autocorrelation function of free Bodipy-FTY720 in a cultured medium (without cells) indicate a diffusion time of 0.21 ± 0.03 ms, which corresponds to a diffusion coefficient of 1.106×10^{-6} cm^2/s. The slight increase in the diffusion coefficient of Bodipy-FTY720 may be attributed to its hydrophobic nature, which may lead to micelles formation.

Representative fluorescence fluctuation autocorrelation curve of sampled Bodipy-FTY720 species in the cultured media (24 hours) and of rhodamine green as a reference are shown in Figure 3:8. In contrast with the single species of rhodamine green in PBS, the autocorrelation function of secreted Bodipy-FTY720 species in the cultured medium is best described with two diffusing species in 3D model. In contrast, the autocorrelation function of the secreted Bodipy-FTY720 indicates a two-diffusing species with distinct slower diffusion coefficients (Figure 3:8, Table 3:3.). For example, the diffusion coefficient of the slowly diffusing Bodipy-FTY720 species (τ_D = 0.50 ± 0.05 ms), secreted in the culture medium, is $(4.6 \pm 0.9)\times10^{-7}$. Assuming the viscosity of water at room temperature, the hydrodynamic radius of such species is ~4.9 nm and therefore distinct from a free Bodipy-FTY720 or its phosphorylated counterpart.

These results imply a larger Bodipy-FTY720 species secreted from the incubated cells into the culture media. One possibility is that such species is exocytosed vesicles observed in the confocal and TIRF experiments, which may contains one or more copies of S1PR-Bodipy-FTY720-P complexes. However, the exact identity of such species remained unknown and is currently under investigation.

Table 3:3 Translational diffusion times of secreted Bodipy-FTY720 in the cultured media of incubated, cultured cells. The systems was calibrated using rhodamine green (6 nM, PBS, pH 7.4) at room temperature.

Sample	Diffusion Time τ_D (ms)	Diffusion Coefficient (cm^2/s)
Secreted Bodipy FTY720 to culture media	0.50 ± 0.05	$(4.6 \pm 0.9)\times10^{-7}$
	0.03 ± 0.02	7.746×10^{-6}
Pure Bodipy-FTY720 in pure culture media	0.21 ± 0.03	$(1.1 \pm 0.8)\times10^{-6}$
Pure Bodipy-FTY720 in ethanol	0.08	2.13×10^{-6}
Rhodamine green in PBS	0.083 ± 0.001	2.8×10^{-6}

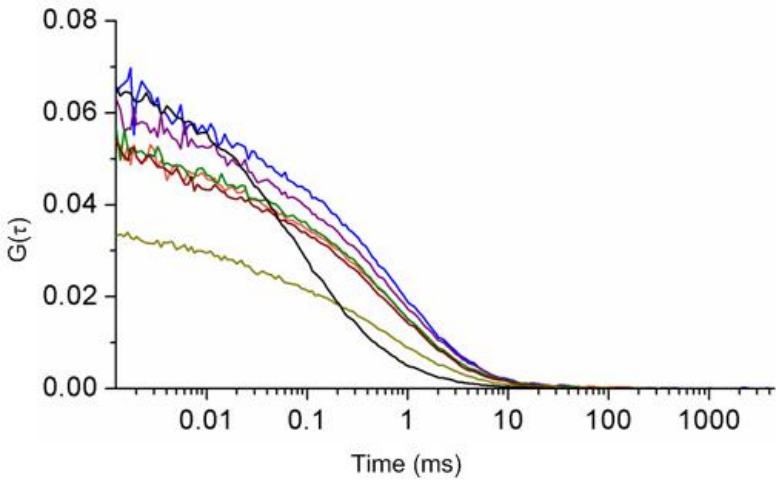

Figure 3:9 Incubation-time-dependent autocorrelation of sampled Bodipy-FTY720 in the culture media of incubated, stained cells. The autocorrelation of secreted Bodipy-FTY720 indicates a slight increase in the number of molecules in the cultured medium with the increase of the incubation time. The blue, violet, green, orange, wine, olive autocorrelation of Bodipy-FTY720 were sampled after 1hr, 2 hr, 3 hr, 4hr, 5 hr, and 24hr of incubation time, respectively. The autocorrelation of rhodamine green (black curve, 6 nM, PBS, pH7.4) is shown as a control.

The time-dependent sampling of the cultured media surrounding adherent cells also reveals an increased number of molecules (Bodipy-FTY720 species) with time (Figure 3:9). The sampled number of molecules reached a plateau after 20 hours and the

overall changes were not drastic. This can be understood in terms of an equilibrium state of Bodipy-FTY720 species between the labeled cells and surrounding cultured media.

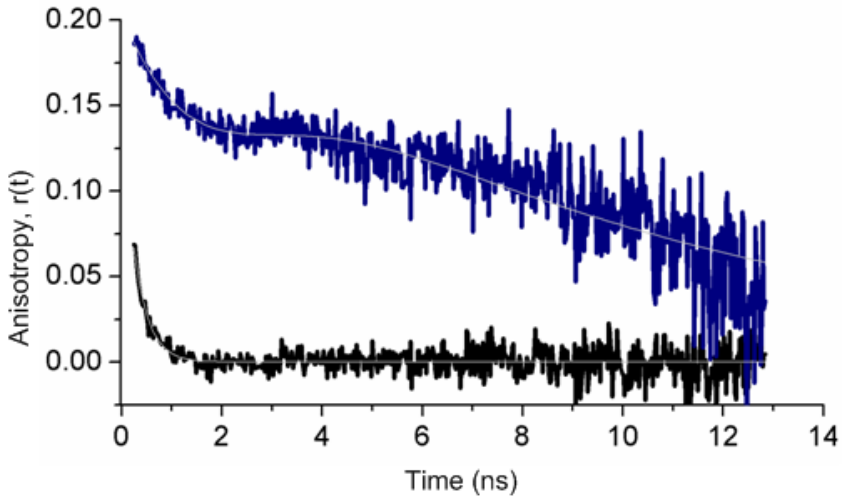

Figure 3:10 The associated anisotropy of sampled Bodipy-FTY720 from the cultured medium indicates the presence of two species with distinct size and fluorescence lifetime. The fitting parameter of associated anisotropy decay on Bodipy-FTY720 is shown in Table 5. In addition, the control anisotropy curve of rhodamine green (1 µM, PBS, pH7.4) is also shown (black curve) with a rotational time of ~120 ps.

To further investigate the flexibility and hydrodynamic radius of the secreted Bodipy-FTY720 species on the nanosecond timescale, we conducted complementary time-resolved anisotropy measurements on the sampled cultured media as described above. Representative anisotropy decays and their fitting parameters are shown in Figure 3:10 and Table 3:4, respectively. For calibration purposes, the anisotropy of rhodamine green (PBS, pH7.4, room temperature) decays as a single exponential with 130 ± 10 ps, which is consistent with its molecular weight (621.05 Da). In contrast, the anisotropy of

the Bodipy-FTY720 species exhibits associated anisotropy nature as described by Equation 2.7.

The observed associated anisotropy of Bodipy-FTY720 species in the cultured media indicates the presence of two tumbling species with distinct sizes and fluorescence lifetimes (Table 3:4 and Figure 3:10). The presence of two different hydrodynamic sizes is consistent with our FCS results. In agreement with our FLIM images, the fluorescence lifetime of ER-membrane bound Bodipy-FTY720 is distinct from those in intracellular vesicles.

As a control, we carried out complementary experiments to examine the fluorescence and size properties of Bodipy-FTY720 in Triton X-100 micelles. Using FCS measurements of fluorescence brightness (the number of fluorescence photons per molecule), we estimated a single Bodipy-FTY720 per micelle. Our FCS results also indicate an estimated size of Bodipy-FTY720-labeled micelles of 7 ± 2 nm at room temperature. In addition, the fluorescence lifetime of Bodipy-FTY720 in micelles (5.86 ns) as compared with 4.92 ns for the free fluorophore in ethanol. Importantly, time-resolved anisotropy of Bodipy-FTY720-labeled micelles indicates that the Bodipy moiety is likely to be in the hydrophobic core of these Triton X-100 micelles.

Taken together, these results combined eliminate the possibility of a single Bodipy-FTY720 in membrane vesicles that are secreted in the culture media. Rather, it is likely that the secreted species in the culture medium may contain membrane vesicles with multiple copies of Bodipy-FTY720 (with or without S1P receptors).

Table 3:4 Fitting parameters for time-resolved associated anisotropy of secreted Bodipy-FTY720 in the cultured medium of incubated, stained cells. The setup was calibrated using rhodamine green (1 μM, PBS, pH 7.4) for G-factor calculations.

Fitting Parameters	Values
α_1	2.8±0.1
τ_1 (ns)	0.82±0.02
α_2	0.021±0.001
τ_2 (ns)	1.20±0.03
β_1	0.10±0.01
φ_1 (ns)	0.59±0.09
β_2	18±2
φ_2 (ns)	2.57±0.03

Chapter 4. Conclusion and Future Outlook

Using multiparametric fluorescence micro-spectroscopy approaches, our results indicate that Bodipy-FTY720 follows a similar pathway as the parent immune modulator FTY720, which is a synthetic analog of sphingosine. According to our time-lapse imaging, Bodipy-FTY720 crosses the plasma membrane of cultured, mouse embryonic C3H10T1/2 cells to reach saturation within minutes. In another words, the Bodipy moiety seems to have negligible effect on the passive transport of Bodipy-FTY720 through the plasma membrane. Importantly, Bodipy-FTY720 partitions in the ER membrane of this cells line where it is expected to be phosphorylated by sphingosine kinase 2. This conclusion is based on the co-localization of Bodipy-FTY720 with the ER Tracker Red™ Dye (Glibenclamide-Bodipy-FL). The time-dependent vesicle formation inside the cells, according to TIRF and time-lapse imaging, seems consistent with the internalization of Bodipy-FTY720-P following its binding with the S1P receptors. The translational diffusion measurements inside the cells confirm the above conclusions concerning Bodipy-FTY720 association with the ER membrane as well as its encapsulation in vesicles. Interestingly, the local environment (ER versus intracellular vesicles) of this fluorescent immune modulator differs according to FLIM measurements. In addition, the time-dependent sampling of the culture media of incubated cells, labeled with Bodipy-FTY720, support our argument that the fluorescently tagged FTY720-P is secreted into the culture media, both as free and bound to the S1P-receptor. The time resolved anisotropy and the translational diffusion studies of bodipy-FTY720 in secreted culture media further supports the idea of phosphorylation of the molecule by ShpK2 and its association to S1P receptors.

Taken together, our results support the hypothesis that Bodipy-FTY720 will be phosphorylated by sphingosine kinase 2 (SphK2) prior to binding to sphingosine-1-phosphate receptor 1 ($S1PR_1$) followed by internalization and degradation. These studies represent a step forward towards new insights into the action mechanism of FTY720 using its fluorescent derivative (Bodipy-FTY720) at the single-cell level.

We are planning to investigate the exocytosis of the Bodipy-FTY720-P-entrapped vesicles using video rate TIRF microscopy. In addition, we will investigate the diffusion dynamics and size characterization of those vesicles using single-particle tracking approach based on TIRF microscope. These studies would provide new insights into degradation mechanism of the Bodipy-FTY720-P-S1P receptor complex. Furthermore, the results will enable us to examine whether each vesicle contains one or multiple copies of these complexes based on our FLIM results. For direct evidence of Bodipy-FTY720-P association with S1P receptors, we are planning to use genetic labeling of those receptors with GFP transformants, which will be chosen for FRET studies based on their spectral overlap with this fluorescently tagged immune modulator. Sphingosine-1-phosphate is a known bioactive signaling molecule that mediates important cellular functions such as cell proliferation, cytoskeletal rearrangement, angiogenesis, mobilization of intracellular calcium and immune cell trafficking. As a result, functional imaging of the S1P and FTY720 derivatives will also be investigated with the context of these biological functions.

Bibliography

1. *Functions of a new family of sphingosine-1-phosphate receptors.* **Sarah Spiegel, Sheldon Milstien.** 2000, Biochimica et Biophysica Acta, Vol. 1484, pp. 107-116.

2. *Different Response Patterns of Several ligands at the Sphingosine-1-phosphate Receptor Sub Type 3 (S1P3).* **Jongsma M, Van Unen J, Van Loenen P B, Michel MC, Peters S L M, Alewinjnse A E.** 2009, British Journal of Pharmacology, Vol. 156, pp. 1305-1311.

3. *An Update on Sphingosine-1-phosphate and other Sphingolipid Mediators.* **Saba, Henrik Fyrst and Julie D.** 2010, nature Chemical Biology, Vol. 6, pp. 489-497.

4. *"Inside-Out" Signaling of Sphingosine-1-Phosphate: Therapeutic Targets.* **Kazuki Takabe, Steven W. Paugh, Sheldon Milstein, Sarah Spiegel.** 2008, Pharmacol Rev, Vol. 60, pp. 181–195.

5. *Role of ABCC1 in export of sphingosine-1-phosphate from mast cells.* **Poulami Mitra, Carole A. Oskeritzian, Shawn G. Payne, Michael A. Beaven, Sheldon Milstien, and Sarah Spiegel.** 2006, PNAS, Vol. 103, pp. 16394–16399.

6. *Critical role of ABCA1 transporter in sphingosine 1-phosphate release from astrocytes.* **Koichi Sato, Enkhzol Malchinkhuu,Yuta Horiuchi, Chihiro Mogi, Hideaki Tomura, Masahiko Tosaka, Yuhei Yoshimoto, Atsushi Kuwabara and Fumikazu Okajima.** 2007, Journal of Neurochemistry, Vol. 103, pp. 2610–2619.

7. *Syntheses of Sphingosine-1-phosphate Stereoisomers and Analogues and Their Interaction with EDG Receptors.* **Hyun-Suk Lim, Yong-Seok Oh, Pann-Ghill Suh and**

Sung-Kee Chung. 2003, Bioorganic & Medicinal Chemistry Letters, Vol. 13, pp. 237–240.

8. *Molecular Recognition in the Sphingosine 1-Phosphate Receptor Family.* **T. Truc-Chi, Pham, James I. Fells Sr., Daniel A. Osborne, E. Jeffrey North, Mor M.** 8, 2008, J Mol Graph Model, Vol. 26, pp. 1189–1201.

9. *FTY720: targeting G-protein-coupled receptors for sphingosine 1-phosphate in transplantation and autoimmunity.* **Volker Brinkmann, Kevin R Lynch.** 14, s.l. : Current Opinion in Immunology, 2002, pp. 569–575.

10. *Fingolimod (FTY720): discovery and development of an oral drug to treat multiple sclerosis.* **Volker Brinkmann, Andreas Billich, Thomas Baumruker, Peter Heining, Robert Schmouder, Gordon Francis, Shreeram Aradhye & Pascale Burtin.** 2010, Nature Reviews Drug Discovery, Vol. 9, pp. 883-897.

11. *FTY720: Altered Lymphocyte Traffic Results in Allograft Protection.* **Brinkmann, Volker, Pinschewer, Daniel D., Feng, Lili, Chen Shizhong.** 5, s.l. : Transplantation, 2001, Vol. 72, pp. 764-769.

12. *Update in Nuerology.* **Florina, Antochi.** s.l. : Medica-A Journal of Clinical Medicine, 2011, Vol. 6, p. 64.

13. *Design, synthesis, and structure-activity relationships of 2-substituted-2-amino-1,3-propanediols: Discovery of a novel immunosuppressant, FTY720.* **Kunitomo Adachi, Toshiyuki Kohara, Noriyoshi Nakao, Masafumi Arita, Kenji Chiba, Tadashi Mishin, Shigeo Sasaki, Tetsuro Fujita.** s.l. : Bioorg. Med. Chem. Lett., 1995, Vol. 5, pp. 853-856.

14. *The immunosuppressant FTY720 is phosphorylated by sphingosine kinase type 2.* **Steven W. Paugh, Shawn G. Payne, Suzanne E. Barbour, Sheldon Milstien and Sarah Spiegel.** s.l. : Federation of European Biochemical Societies, 2003, Vol. 554, pp. 189-193.

15. *The Immune Modulator FTY720 Targets Sphingosine 1-Phosphate Receptors.* **Volker B., Michael D. D., Christopher E. H., Rainer A., Sylvain C., Robert H., Christian B., Eva P., Thomas B., Peter H., Carolyn A. F, Markus Z., and Kevin R. L.** 2002, The Journal of Biological Chemistry, Vol. 277, pp. 21453–21457.

16. *Novel immunomodulator FTY720 is Phosphorylated in Rats and Humans To Form a Single Sterioisomer. Identification, Chemical Proof, and Biological Active Species and Its Enantiomer.* **Rainer A., Klaus H., Volker B., Danilo G., Muller-Hartwieg, Helmut K., Corinne S., Markus S, Trixie W., Karl W., Frederic Z., Markus Z., Nigel C. and Eric F.** s.l. : J. Med. Chem, 2005, Vol. 48, pp. 5373-5377.

17. *Synthesis of para-alkyl aryl amide analogues of sphingosine-1-phosphate: discovery of potent S1P receptor agonists.* **Clemens J.J., Davis M.D., Lynch K.R., Macdonald T.L.** 2003, Bioorg Med Chem Lett, Vol. 13, pp. 3401-3404.

18. *Fingolimod (FTY720): A Recently Approved Multiple Sclerosis Drug Based on a Fungal Secondary Metabolite.* **Cherilyn R. Strader, Cedric J. Pearce, and Nicholas H. Oberlies.** 2011, Journal of Natural Products, Vol. 74, pp. 900–907.

19. *CYP4F Enzymes Are Responsible for the Elimination of Fingolimod (FTY720), a Novel Treatment of Relapsing Multiple Sclerosis.* **Jin Y., Zollinger M., Borell H., Zimmerlin A., Patten C.J.** 2010, S. Drug Metab. Dispos., Vol. 39, pp. 199-207.

20. *Synthesis and spectral properties of cholesterol- and FTY720-containing boron dipyrromethene dyes.* **Li, Z., and Bittman, R.** s.l. : J. Org. Chem., 2007, Vol. 72, pp. 8376–8382.

21. *Membrane fluidity and lipid order in ternary giant unilamellar vesicles using a new Bodipy-cholesterol derivative.* **Ariola, F.S., Li, Z., Cornejo, C., Bittman, R., and Heikal, A.A.** s.l. : Biophysical Journal, 2009, Vol. 96, pp. 2696–2708.

22. *Membrane order and molecular dynamics associated with IgE receptor cross-linking in mast cells.* **Davey, A.M., Walvick, R.P., Liu, Y., Heikal, A.A., and Sheets, E.D.** s.l. : Biophys. J., Vol. 92, pp. 343-355.

23. *Integrated biophotonics approach for non-invasive, multiscale studies of biomolecular and cellular biophysics.* **Yu, Q., Proia, M., and Heikal, A.A.** s.l. : J. Biomed. Opt., 2008, Vol. 13.

24. *Synthesis and spectral properties of Cholesterol- and FTY- Containing Boron Dipyrromethene Dyes.* **Zaiguo Li, Robert Bittman.** 2007, J. Org. Chem., Vol. 72, pp. 8376-8382.

25. *Ceramide Conversion to Sphingosine-1-Phosphate is Essential for Survival in C3H10T1/2 Cells.* **Teegarden, S. Sianna Castillo and Dorothy.** s.l. : American Society for Nutritional Sciences, 2001.

26. *Confirmational Dependence of Intracelluar NADH on Metabollic State Revealed by Associated Fluorescence Anisotropy.* **Harshad D.Vishwasrao., Ahmed A. Heikal, Karl A.Kasischke, Watt W. Webb.** 2005, The Journal of Biological Chemistry, Vol. 280, pp. 25119-25126.

27. **Lackowicz, Joseph R.** *Principles of Fluorescence Spectroscopy.* s.l. : Springer.

28. *Dynamics Imaging of lipid phases and lipid marker interaction in model biomembranes.* **F.S. Ariola, D.J. Mudadliar, R.P. Walvick and A.A. Heikal.** s.l. : Phys.Chem.Chem.phys., 2006, Vol. 8, pp. 4517-4529.

29. *Integrated Biophotonics approach for Noninvasive and Multiscale Studies of Biomolecular and cellular biophysics.* **Qianru Yu, Michael Proia, Ahmed A. Heikal.** 2008, Journal of biomedical Optics, Vol. 13.

30. *Two-photon Autofluorescence Dynamics Imaging Reveals Sensitivity of Intracellular NADH Concentration and Confirmation to Cell Physiology at the Single-cell Level.* **Qianru Yu, Ahmed A. Heikal.** 2009, Journal of photo chemistry and photobiology, Vol. 95, pp. 46-57.

31. *Fluorescence Correlation Spectroscopy: the technique and its applications.* **Bonnet, Oleg Krichevsky and Gregoire.** 2002, Reports On Progress in Physics, Vol. 65, pp. 251-297.

32. *Anomalous Diffusion of Proteins Due to Molecular Crowding.* **Jedrzej Szymanski, Matthias Weiss.** 2005, physical review Letters, Vol. 103.

33. *Mapping of fluorescence anisotropy in living cells by ratio imaging, Application to cytoplasmic viscosity.* **James A. Dix, A. S. Verkman.** 1990, Biophys. J., Vol. 57, pp. 231-240.

34. *FTY720 Stimulates 27-Hydroxycholesterol Production and Confers Atheroprotective Effects in Human Primary Macrophages.* **Tomas Blom, Nils Bäck, Aino-Liisa Mutka,**

Robert Bittman, Zaiguo Li, Angel de Lera, Petri T. Kovanen, Ulf Diczfalusy and Elina Ikonen. s.l. : American Heart Association, 2010, Circulation Research, pp. 720-729.

35. *Membrane fluidity and lipid order in ternary giant unilamellar vesicles using a new Bodipy-cholesterol derivative.* **Ariola, F.S., Z. Li, C. Cornejo, R. Bittman, and A.A. Heikal.** 2009, Biophysical Journal, Vol. 96, pp. 2696-2708.

Appendices – Laboratory Protocols

Cell Culture

C3H10T1/2 Culture Media - Recipe for one 500 mL Bottle

- Eagle's Basal Medium (BME) - (500 mL less 65 mL)
- Heat Inactivated FBS (10%) - (50 mL)
- Sodium Bicarbonate (7.5% w/v%) - 11 mL
- Penicillin-Streptomycin - 5.5 mL

  (Penicillin - 100U/ mL medium & Streptomycin - 100mg/ mL medium)

Staining C3H10T1/2 Cells with Bodipy-FTY720

I. The C3H10T1/2 cells are plated in 35 mm MatTek dishes at 1.2×10^5 cells/mL 24hrs before staining.

II. Before staining the cells, they are replaced with new 2mL of culture media.

III. Staining.

   A. For <u>imaging</u> purposes, following are the volumes used to add in to the 2mL of culture media.

   - LZ532C – 1.5 µL of 1.50 mM stock solution (to achieve ~1.125 µM/ 2mL of culture media)
   - LZ570 – 1.2 µL of 1.90 mM stock solution (to achieve ~1.125 µM/ 2mL of culture media)

   B. For <u>FCS</u>

- LZ532C – 0.27 µL of 0.15 mM stock solution (to achieve ~20 nM/ 2mL of culture media)
- LZ570 – 0.21 µL of 0.19 mM stock solution (to achieve ~20 nM/ 2mL of culture media)

C. For <u>Anisotropy</u>

- LZ532C –2.7 µL of 0.15 mM stock solution (to achieve ~20 µM/ 2mL of culture media)
- LZ570 –2.1 µL of 0.19 mM stock solution (to achieve ~20 µM/ 2mL of culture media)

IV. Then the dish is incubated for 10 min at 37°C.

V. After incubation, the staining solution is washed with 2mL Tyrode's buffer, five times carefully.

VI. Replace with 2 mL of Tyrode's buffer for the experiment.

VII. The dish will only be good for ~1.5 hrs.